

Synthesis of Stochastic Representations of Ground Motions

By S. C. LIU

(Manuscript received December 4, 1969)

In this paper, we study a number of stochastic models including stationary, nonstationary, and linear processes for the purpose of simulating earthquake- or explosion-induced ground motions. The important statistical characteristics of each model and their effects on structural systems are investigated in some detail. We obtain expressions for the mean-square response of simple linear mass-spring oscillators to each model. We discuss numerical procedures for time series simulations of these models. The objectives of this paper are (i) to examine and compare the statistical properties and effects on structures of all possible stochastic processes applicable to model ground motions and (ii) to offer engineers a basis for forming their own judgments.

I. INTRODUCTION

A primary concern in problems dealing with earthquake or blast response is the proper definition of random force environments. Typical problems include the design of earthquake-resistant frames for electronic or mechanical facilities in a building, and the estimation of structural damage resulting from nuclear detonation in a given area. Normally it is necessary to create ground-motion data artificially from information derived from limited recordings. Therefore, in ground-motion analysis, as in many other fields of engineering physics, time series modeling or simulation problems emerge. This paper carries forward the concern with such problems.

In a previous paper the statistical characteristics of a collection of earthquake ground-motion data were analyzed.¹ It was shown that a stationary random process of finite duration could be used to model the high-intensity phase of a ground-motion accelerogram. It was suggested that a narrowband stationary process be used. However, the narrowband process, like many other stationary models, fails to produce

the initial buildup and the decaying terminations which are apparent in many real ground-motion accelerograms. To simulate these portions, nonstationary models must be used. In this paper we investigate a number of physically realizable stationary, nonstationary, and linear stochastic models, when applicable to the simulation of ground motions. We derive the important statistics of these models and discuss numerical simulation procedures. The covariance, autocorrelation function, and power spectral density of the response process of a class of linear time-invariant systems excited by the input process represented by each model are examined. It is hoped that by comparing these models for basic definition, for simulation procedure, and for effects on induced structural responses, a practicing engineer will be able to select one that will be suitable for the analysis of his specific problem. It is the intent of this paper not only to sum up the current state of the art/science but also to give to researchers in the field of ground motion study such hints and directions for the development of advanced stochastic models as mathematical sophistication permits.

II. STOCHASTIC MODELS

2.1 *Stationary Models*

A typical ground-motion accelerogram from an earthquake or nuclear detonation consists of three phases: an initial rapid-buildup phase, a high-intensity primary phase, and a gradually decaying tail—all obviously nonstationary phenomena. However, many researchers still prefer to model earthquakes by stationary processes because the low-amplitude starting and ending portions of an accelerogram do not significantly affect the structural response as compared with the response induced by the primary phase. Therefore it appears legitimate to model the primary phase by a stationary process of finite duration. Furthermore, the stationariness assumption greatly simplifies the response evaluations and numerical simulation procedures. This feature is particularly important from the practical viewpoint. Three stationary models, designated as $x_1(t)$, $x_2(t)$, and $x_3(t)$, along with their autocorrelation function and power spectral density are defined in Table I.

The first model, white noise $x_1(t)$, defined as a stationary random signal having gaussian probability amplitude distribution and a constant spectral density for all frequencies, is the simplest one of all. Numerically, it can be simulated by generating a sequence of gaussian independent samples of gaussian random numbers g_n , spacing them at small time interval Δt , and assuming linear variation between amplitudes

TABLE I—STATIONARY MODELS AND CORRESPONDING AUTOCORRELATION AND SPECTRAL DENSITY FUNCTIONS

MODEL	I	II	III
NAME	White Noise	Filtered White Noise	Impulse Process
Definition, $x(t)$	$x_1(t)$	$x_2(t) = \int_{-\infty}^{\infty} h_0(t - \tau)x_1(\tau)d\tau$	$x_3(t) = \sum_{n=-\infty}^{\infty} a_n\delta(t - t_n)$
Autocorrelation Function, $R_x(\tau)$	$2\pi S_0\delta(\tau)$	$2\pi S_0 \int_0^{\infty} h_0(t)h_0(t + \tau)d\tau$	$\beta \left[\rho(0)\delta(\tau) + \sum_{n=1}^{\infty} \rho(n)p_n(\tau) \right]$
Spectral Density Function, $S_x(\omega)$	S_0	$ H_0(i\omega) ^2 S_0$	$\beta \left[\rho(0) + 2Re \sum_{n=1}^{\infty} \rho(n)P_n(i\omega) \right]$

over each Δt . Bycroft² has studied this overly simplified model on an analog computer. This model fails to provide any frequency descriptions of the motions that are so important to the structural response analysis; its use results solely from its mathematical simplicity.

For model $x_2(t)$, the filtered white noise, symbols $h_0(t)$ and $H_0(\omega)$ in Table I represent the transfer function in the time and frequency domains, respectively. The process $x_2(t)$ is a gaussian, covariance stationary, narrowband process. The use of $x_2(t)$ in modeling earthquake ground motions is based upon the resemblance of the autocorrelation function, the power spectral density, and the response spectra of strong motion earthquakes to those of the narrowband process.^{1,3,4} The numerical simulation of $x_2(t)$ based on prescribed power spectral density is a routine exercise using the basic relationship between the power spectral densities $S_{x_1}(\omega)$ and $S_{x_2}(\omega)$ of the input and output of the linear filter:

$$S_{x_2}(\omega) = |H_0(\omega)|^2 S_{x_1}(\omega). \quad (1)$$

This equation suggests that a signal $x_2(t)$ can be created from the random process $x_1(t)$ whose spectral density $S_{x_1}(\omega) \equiv 1$ by passing $x_1(t)$ through a filter whose transfer function $H_0(\omega)$ satisfies $|H_0(\omega)|^2 = S_{x_2}(\omega)$. A detailed approach to simulating stationary processes with a rational spectral density function, which is represented by a quotient of two polynomials in ω , has been described by Franklin.⁵ Methods of estimating ground-motion spectral densities are given by Liu and Jhaveri.^{1,4} A sample function of process $x_2(t)$, generated digitally by passing a white noise through a linear filter with a natural frequency of 10 rad/s and a damping ratio of 5 percent, is shown in Fig. 1 which demonstrates a typical appearance of a narrowband process. The justification for using this process to model ground motions is that both its power spectral density function and its response spectrum resemble and can be made to match those of real-world records. It reflects the predominant effects of the site on motion and, by using a modal analysis, $x_2(t)$ can model ground motions which exhibit multiple peaks in their frequency spectrograms.⁴

For $x_3(t)$ as defined in Table I the random impulses $\{a_n\}$ form a stationary discrete parameter process, and $\{t_n\}$ is a stationary point process independent of $\{a_n\}$.^{6,7} As in the expressions for autocorrelation function and power spectral density, β is the average number of impulses per unit time interval and $p_n(t)$ represents the probability density function for n consecutive intervals of $\{t_n\}$ within a time duration t ; $\rho(n)$ and $P_n(i\omega)$ are defined as

$$\rho(n) = E[a_m a_{m+n}] \quad (\text{any } m) \quad (2)$$

$$P_n(i\omega) = \int_0^\infty p_n(t) \exp(-i\omega t) dt \quad (3)$$

in which $E[\]$ denotes ensemble averages.

Notice that the model $x_3(t)$ allows correlation $\rho(n)$ to exist among the random amplitudes a_n which are assumed to be independent for many other stochastic models. The simulation of $x_3(t)$ can be achieved by the spectral approach as described by Franklin or by the correlation approach based on the matrix factorization procedure as proposed by Moore and Anderson.⁸ However, when $p_n(t)$ is poisson with mean arrival rate β and Markov correlation $\rho(n) = \rho^{|n|}$ and $|\rho| \leq 1$, a sample function of $x_3(t)$ can be created by simultaneous simulations of independent samples of $\{a_n\}$ and $\{t_n\}$. In this case the probability density function of the waiting time $\tau_k = t_{k+1} - t_k$ is an exponential distribution, that is, $p(\tau_k) = \beta \exp(-\beta\tau_k)$ and therefore a sequence τ_k can be generated from a sequence of uniformly distributed random numbers w_k :

$$\tau_k = -\frac{1}{\beta} \ln(1 - w_k), \quad 0 \leq w_k < 1. \quad (4)$$

The correlation $\rho^{|n|}$ can be introduced into $\{a_n\}$ by using an autoregressive transformation of a sequence of gaussian random numbers g_n with zero mean and unit variance:

$$\begin{aligned} a_n &= (1 - \rho^2)^{\frac{1}{2}} a'_n \\ a'_n &= \rho a'_{n-1} + g_n. \end{aligned} \quad (5)$$

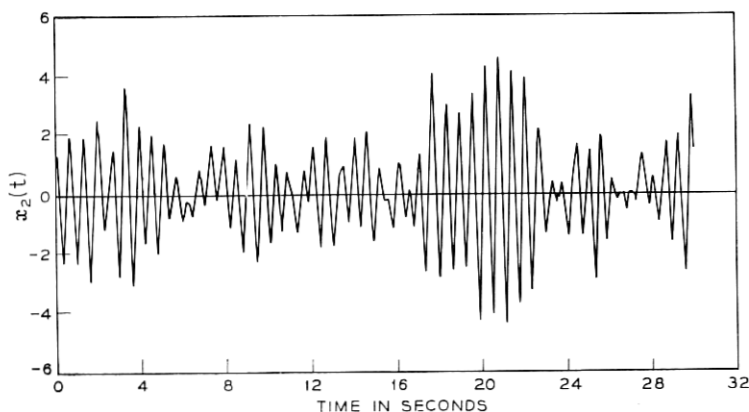


Fig. 1—Sample function of process $x_2(t)$.

A digitally simulated sample of $x_3(t)$ with $\rho = 0.5$, $\beta = 1.0$, and poisson distribution for $p_n(\tau)$ is shown in Fig. 2(a); its autocorrelation function and power spectral density are shown, respectively, in Figs. 2(b) and (c). The time response of a linear filter having a natural frequency $\omega = 10.0$ rad/s and a damping ratio $\zeta = 5$ percent to this input sample member of $x_3(t)$ is shown in Fig. 3(a). The corresponding autocorrelation function and power spectral density of the sample response are shown in Figs. 3(b) and (c), respectively. Notice that Fig. 3(b) exhibits a damped oscillatory motion with a frequency $\omega = 10.0$ rad/s which is the natural frequency of the filter. At this frequency there is a peak in the power spectral density as shown in Fig. 3(c) which is similar to that of strong-motion earthquakes. Notice also that in comparison with $x_3(t)$, which shows abrupt peaks and dips in the waveform, the filtered impulse process more closely resembles a ground-motion accelerogram. Based on these results, it appears that a filtered impulse process may be more appropriate than the impulse process $x_3(t)$ itself in modeling earthquake motions.

When ground motions are represented by stationary processes, it is extremely important to properly determine the duration and intensity of the processes because the induced response of structures depends heavily on these two parameters. To those who are reluctant to neglect the nonstationary effect resulting from the starting and tail portions of earthquake accelerograms, the stationary models I through III obviously are not satisfactory. One might therefore consider using the following nonstationary models.

2.2 Nonstationary Models

Five useful nonstationary models, $x_4(t)$ through $x_8(t)$, are defined in Table II.

The model $x_4(t)$ is a frequency-modulated nonstationary function. For its definition in Table II, b_i , α_i , and ω_i are given sets of real positive numbers, and w_i are independent random variables from uniform distribution over 0 and 2π . The use of $x_4(t)$ is based on the result that the skewed bell shape covariance function of $x_4(t)$ is similar to and can be made to match that of an earthquake. Numerical simulations of $x_4(t)$ present no special difficulty as its sample members can be created directly for given sets of b_i , α_i , and ω_i according to its definition. It may be expected that use of a large number of terms as given by $x_4(t)$ will produce member functions that look much more like real earthquake accelerograms.⁹

For the model $x_5(t)$, $\phi(t)$ is a deterministic or envelope function and

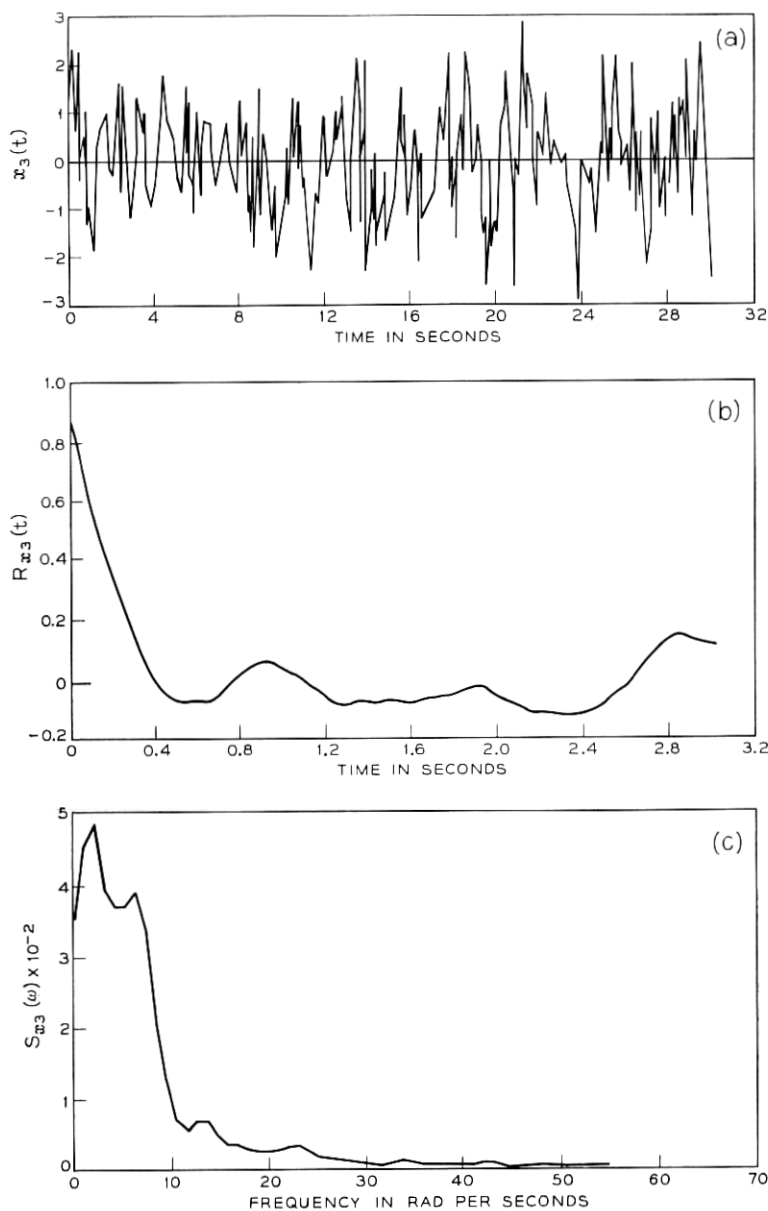


Fig. 2(a)—Digital realization of sample $x_3(t)$, the impulse process.

Fig. 2(b)—Autocorrelation function of sample $x_3(t)$.

Fig. 2(c)—Power spectral density function of sample $x_3(t)$.

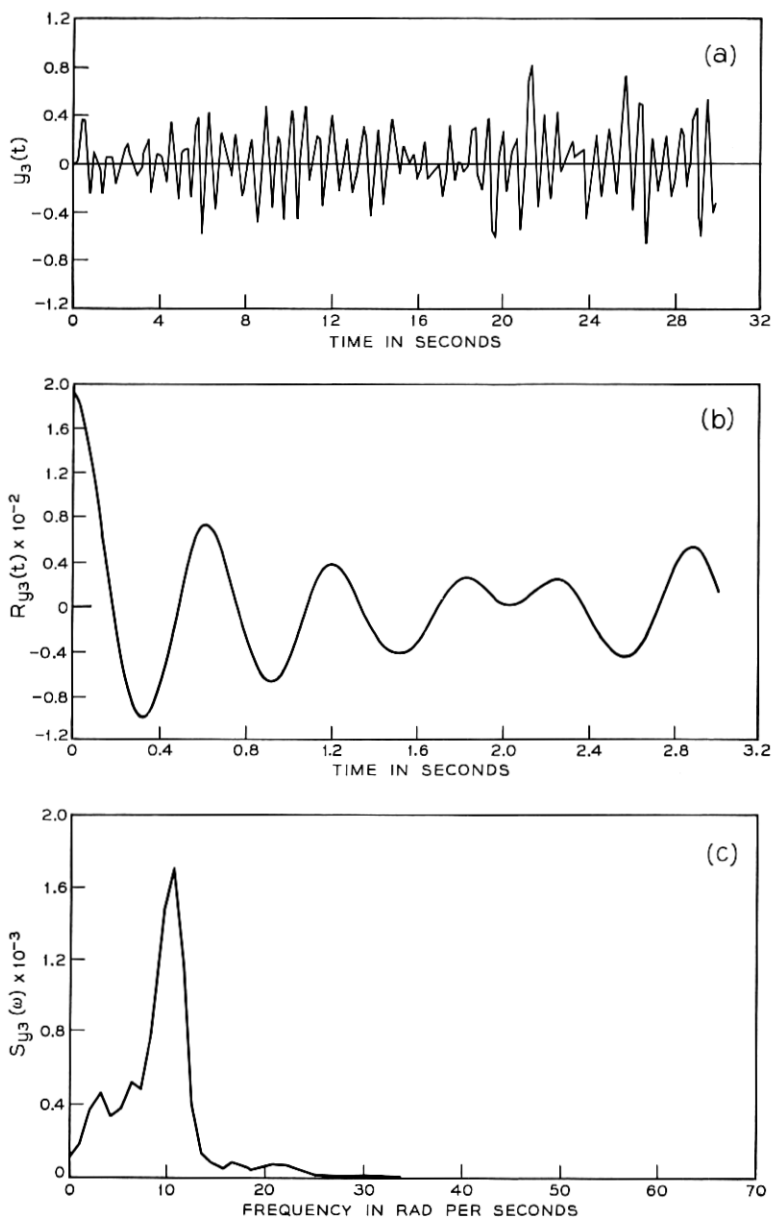


Fig. 3(a)—Digital realization of sample response of $x_3(t)$.

Fig. 3(b)—Autocorrelation function of sample response of $x_3(t)$.

Fig. 3(c)—Power spectral density function of sample response of $x_3(t)$.

TABLE II—DEFINITION OF NONSTATIONARY MODELS

MODEL	NAME	DEFINITION
IV	Frequency Modulated Random Function	$x_4(t) = \sum_{j=1}^n lb_j \exp(-\alpha_j t) \cos(\omega_j t + w_j)$
V	Separable Nonstationary Process	$x_5(t) = \phi(t)f(t)$
VI	Filtered Separable Nonstationary Process	$x_6(t) = \int_{-\infty}^{\infty} h_0(t - \tau)x_5(\tau)d\tau$
VII	Shot Noise	$x_7(t) = \sum_r a(t_r)\delta(t - t_r)$
VIII	Filtered Shot Noise	$x_8(t) = \sum_k a_k h_0(t - t_k)$

$f(t)$ is a stationary random process with given autocorrelation function and power spectral density. The function $f(t)$ may be any one of processes $x_1(t)$, $x_2(t)$, and $x_3(t)$. This model in its various forms has been studied by Peterson and Pullen^{10,11} and by MacNeal, and others.¹² The process $x_5(t)$ has been suggested for model earthquake motions by Shinozuka and Sato¹³ and by Jennings, and others.¹⁴ The process $x_6(t)$ is the response function of $x_5(t)$. In Fig. 4 is shown a sample member of $x_5(t)$ with $\phi(t) = \sin(\pi t/30)$ and $f(t)$ as the sample member of $x_2(t)$ in Fig. 1. Its response function to a linear filter with a natural frequency of 10 rad/s and a damping ratio of 5 percent is shown in Fig. 5 which represents a sample of the process $x_6(t)$. Figure 4 clearly illustrates that the waveform is enveloped by a half-sine wave which produces a strong phase between the times of 17 and 23 seconds. The high-amplitude tail observed in Fig. 5 is obviously undesirable in modeling ground motion. However, notice that this figure shows only the response history cutoff at the end of excitation. If free vibration is allowed after the termination of the input, the highly amplified portion will gradually decay, and the resulting waveform will then compare more favorably with real ground-motion records as shown.

A nice feature of process $x_5(t)$ is its separable property which greatly simplifies the mathematics required to evaluate the response statistics. Furthermore, the envelope function $\phi(t)$ can be chosen so that the pattern of the rise and fall of the simulated waveforms is similar to that of a real earthquake motion. However, because the choice of $\phi(t)$ is arbitrary, when using $x_5(t)$ the associated nonstationary effects resulting from the

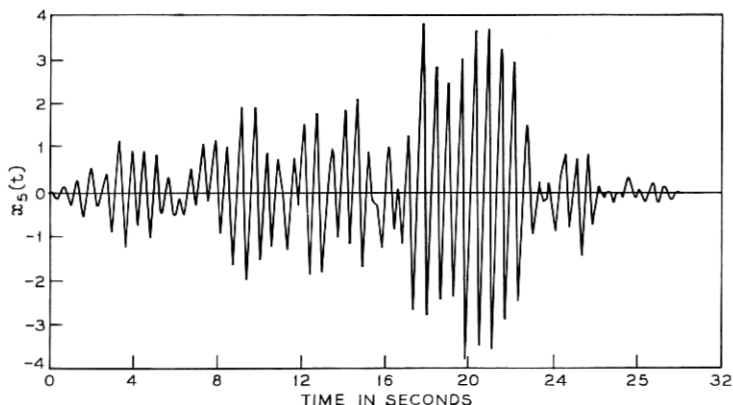
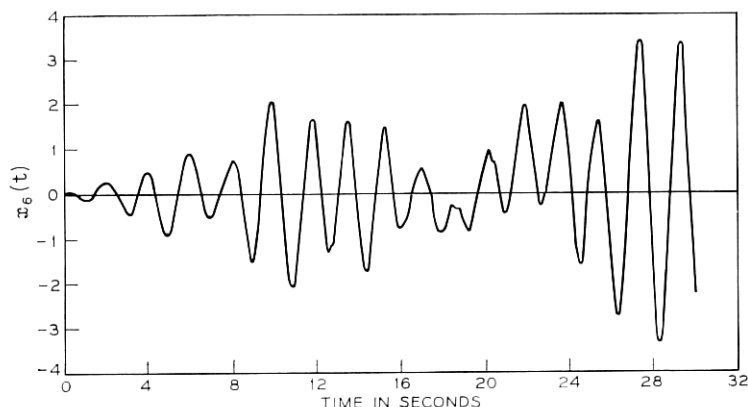


Fig. 4—Sample function of process $x_5(t)$.

Fig. 5—Sample function of process $x_6(t)$.

total time duration, the time proportion of the three distinct phases of the ground motion, and the rate of buildup and decay must be carefully examined.

The shot noise $x_7(t)$ and the filtered shot noise $x_8(t)$ are the nonstationary counterparts of the stationary white noise $x_1(t)$ and filtered white noise $x_2(t)$, respectively. The nonstationariness is introduced into these models by two sources: the time-dependent mean arrival rate $\beta(t)$ and the time-dependent amplitude joint probability density function $p(a_i, t_i; a_j, t_j)$. However, it is assumed that the impulse amplitudes are completely uncorrelated, that is, the joint probability density function is separable:

$$p(a_1, t_1; a_2, t_2) = p(a_1, t_1)p(a_2, t_2).$$

Further, the probability of n impulses in a small interval dt is negligible for $n \geq 2$. Based upon these conditions, it can be shown that the covariance functions of $x_7(t)$ and $x_8(t)$ are also time-dependent:

$$\text{Cov}_{x_8}(t_1, t_2) = \int_{\Gamma} h_0(t_1 - \tau)h_0(t_2 - \tau)E[a^2(\tau)]\beta(\tau) d\tau; \quad (6)$$

$$\begin{aligned} \text{Cov}_{x_7}(t_1, t_2) &= \int_{\Gamma} \delta(t_1 - \tau) \delta(t_2 - \tau)E[a^2(\tau)]\beta(\tau) d\tau \\ &= E[a^2(t_1)]\beta(t_1) \delta(t_1 - t_2) \\ &= I(t_1) \delta(t_1 - t_2); \end{aligned} \quad (7)$$

where Γ denotes the appropriate time domain, and $I(t)$ is the strength

function of the shot noise defined as

$$E[x_7(t)x_7(t + \tau)] = I(t) \delta(\tau).$$

Notice that, when $I(t)$ is a constant, both $x_7(t)$ and $x_8(t)$ become stationary.

The process $x_7(t)$ can be constructed by generating independent gaussian random variables a_n with zero mean and variance equal to $I(t_n) \Delta t$, and by linearly connecting them over Δt along the time axis. The process $x_8(t)$ can be obtained in a similar way simply by shaping each impulse with the transfer function $h_0(t)$ according to its definition in Table II. Amin and Ang¹⁵ have used process $x_8(t)$ with a second-order filter to model earthquakes. Both $x_7(t)$ and $x_8(t)$ are justified on the basis of the similarity between real and nonstationary waveforms and on the matching (i) of their time-varying covariance functions and (ii) of the induced response spectra with those of the real ground-motion data.

2.3 Linear Models

Special cases of the mixed autoregressive-moving average process x_t of order (m, n) as defined below also can be used to model ground motions:

$$x_t = \sum_{i=1}^m \phi_i x_{t-i} + g_t + \sum_{i=1}^n \theta_i g_{t-i}, \quad t = 0, \pm 1, \pm 2, \dots \quad (8)$$

where ϕ_i and θ_i are characterization parameters, and process $\{g_t\}$ is a white noise. An m -order autoregressive (ar) process is given by the first sum of equation (8), that is,

$$x_t = \sum_{i=1}^m \phi_i x_{t-i} + g_t \quad (9)$$

and an n -order moving average (ma) process by the second sum

$$x_t = g_t - \sum_{i=1}^n \theta_i g_{t-i}. \quad (10)$$

The ar processes given in equation (9) are particularly useful in time series simulations because they are very flexible and can be used to model a wide range of real-world random data. For example, the autocorrelation function of a second-order ar process, involving only two parameters, can produce a wide variety of autocorrelation functions. Therefore by matching the ground-motion autocorrelation function of the damped oscillatory type, one can estimate parameters ϕ_i and fit the observed motion to an appropriate linear stochastic model.

III. RESPONSE ANALYSIS

Because a ground-motion model when chosen will be used to specify vibration environments for structural testing and design, it is important to examine its effects on the time and frequency response of some representative systems. In what follows we shall compute and compare the mean-square response of a class of second-order linear systems to stochastic inputs represented by models as described in the previous section. The linear systems are characterized by two constant parameters, the damping coefficient ζ and a natural frequency ω_n , and have transfer functions

$$\begin{aligned} h(t) &= \frac{\exp(-\zeta\omega_n t)}{p} \sin pt, & t \geq 0; \\ &= 0 & t < 0; \end{aligned} \quad (11)$$

where $p = \omega_n(1 - \zeta^2)^{\frac{1}{2}}$.

Let the response function to $x_i(t)$ be $y_i(t)$; $i = 1, 2, \dots, 8$, for systems defined by equation (11). The mean-square response is given by

$$E[y_i(t)^2] = \int_{\Gamma} \int_{\Gamma} h(t - \tau) h(t - \tau') g_i(\tau, \tau') d\tau d\tau', \quad i = 1, 2, \dots, 8. \quad (12)$$

The function $g_i(\tau, \tau')$ for each model is

$$\begin{aligned} g_1 &= 2\pi S_0 \delta(\tau - \tau'), \\ g_2 &= R_{x2}(\tau - \tau') = 2\pi \int_0^{\infty} h_0(t) h_0(t + \tau - \tau') dt, \\ g_3 &= R_{x3}(\tau - \tau') = \beta \left[\rho(0) \delta(\tau - \tau') + \sum_{n=1}^{\infty} \rho(n) p_n(|\tau - \tau'|) \right], \\ g_4 &= \frac{1}{2} \sum_1^n \tau \tau' a_i^2 \exp(-\alpha_i(\tau + \tau')) \cos \omega_i(\tau' - \tau), \\ g_5 &= \phi(\tau) \phi(\tau') R_f(\tau - \tau'), \\ g_6 &= \int_{\Gamma} \int_{\Gamma} h_0(\tau - \theta_1) h_0(\tau' - \theta_2) \phi(\theta_1) \phi(\theta_2) R_f(\theta_2 - \theta_1) d\theta_1 d\theta_2, \\ g_7 &= E[a^2(\tau)] \beta(\tau) \delta(\tau - \tau') = I(\tau) \delta(\tau - \tau'), \\ g_8 &= \int_{\Gamma} h_0(\tau - \theta) E[a(\theta)] \beta(\theta) d\theta \int_{\Gamma} h_0(\tau' - \theta) E[a(\theta)] \beta(\theta) d\theta \\ &\quad + \int_{\Gamma} h_0(\tau - \theta) h_0(\tau' - \theta) E[a^2(\theta)] \beta(\theta) d\theta. \end{aligned} \quad (13)$$

The explicit expression for the mean-square response to stationary models can be obtained by integrations using equations (11) through (13):

$$\begin{aligned}
 E[y_1^2(t)] &= \frac{\pi S_0}{2\zeta\omega_n^2} + \frac{\pi S_0}{2p^2\omega_n} \\
 &\quad \cdot (\zeta \cos 2pt - (1 - \zeta^2)^{\frac{1}{2}} \sin 2pt - 1/\zeta) \exp(-2\zeta\omega_n t), \quad (14) \\
 E[y_2^2(t)] &\simeq \frac{\pi S_{x_2}(\omega_n)}{2\zeta\omega_n^3} \\
 &\quad \cdot \left[1 - \frac{\exp(-2\omega_n \zeta t)}{p^2} \{p^2 + 2(\omega_n \zeta)^2 \sin^2 pt + \omega_n p \zeta \sin 2pt\} \right]. \quad (15)
 \end{aligned}$$

It is assumed in equation (15) that $S_{x_2}(\omega)$, the power spectral density of $x_2(t)$, is given, and the main contribution of $x_2(t)$ to the response comes from the region around $\omega = \omega_n$.¹⁶ And:

$$\begin{aligned}
 E[y_3^2(t)] &= \beta c_1 + \beta \exp(-2\zeta\omega_n t) \left[c_2 \cos 2pt + c_3 \sin 2pt \right. \\
 &\quad + \frac{\beta\rho}{p^2} (\zeta^2\omega_n^2 - a^2) \sin^2 pt + \frac{\beta\rho}{\gamma} \cos^2 pt - \frac{\beta\rho a\mu}{2p^2\zeta\omega_n} \Big] \\
 &\quad - \frac{2\beta^2\rho}{p\gamma} \exp(-(\zeta\omega_n + a)t) [(a + \zeta\omega_n) \sin pt + p \cos pt] \quad (16)
 \end{aligned}$$

in which $a = (1 - \rho)\beta$, $\mu = a^2 + (1 - 2\zeta^2)\omega_n^2$, $\gamma = (a^2 + \omega_n^2)^2 - 4a^2\zeta^2\omega_n^2$, and

$$\begin{aligned}
 c_1 &= \frac{\beta\rho}{\gamma} \left(1 + \frac{a\mu}{2\zeta\omega_n^3} - \frac{a\zeta}{\omega_n} \right) + \frac{1}{4\zeta\omega_n^3} \\
 c_2 &= \frac{1}{\omega_n} \left[\frac{1}{2p^2} \left(\frac{a\beta\rho\zeta\mu}{\gamma} - \frac{1}{2\zeta} \right) + \frac{a\beta\rho\zeta}{\gamma} \right] \\
 c_3 &= \frac{1}{p} \left[\frac{\beta\rho\zeta}{\gamma} (\omega_n + a\zeta) - \frac{1}{2\omega_n^2} \left(\frac{1}{2} + \frac{a\beta\rho\mu}{\gamma} \right) \right].
 \end{aligned}$$

Notice that, as time increases, mean-square response to each of three stationary models approaches its steady-state level, that is,

$$\lim_{t \rightarrow \infty} E[y_i^2(t)] = \begin{cases} \frac{\pi S_0}{2\zeta\omega_n^3}, & i = 1 \\ \frac{\pi S_{x_2}(\omega_n)}{2\zeta\omega_n^3}, & i = 2 \\ \beta c_1, & i = 3. \end{cases} \quad (17)$$

Let the rate of convergence of the mean-square response be defined as

$$\epsilon_i = \frac{\lim_{t \rightarrow \infty} E[y_i^2(t)] - E[y_i^2(t)]}{\lim_{t \rightarrow \infty} E[y_i^2(t)]} \quad (18)$$

and $N = \omega_n t / 2\pi$ be the number of cycles of the motion required to reach ϵ_i . A lower bound to the estimate of N can be easily established for processes $x_1(t)$ and $x_2(t)$ as the following:

$$N \geq \frac{1}{4\pi\zeta} \ln \left[\frac{1 + \zeta^2 + \zeta(1 - \zeta^2)^{\frac{1}{2}}}{(1 - \zeta^2)\epsilon} \right], \quad 0 < \zeta < 1. \quad (19)$$

From this it is noted that N is independent of the natural frequency ω_n of the system but is heavily dependent on the damping ratio ζ . Figure 6 shows that systems with high damping, when excited by $x_1(t)$ and $x_2(t)$, will approach steady-state level faster than those with low damping. A system with 10 percent damping will reach 90 percent of its steady-state response in two cycles of motion.

Because the mean-square response to $x_3(t)$ involves more parameters than that to $x_1(t)$ or $x_2(t)$, the response convergence rate for $x_3(t)$ is more difficult to evaluate. However, ζ remains as the dominant factor, not β or ρ . The mean-square response of $x_3(t)$, as of $x_1(t)$ and $x_2(t)$, approaches its steady-state value rapidly when ζ is high, slowly when ζ is low.

Explicit expression for the mean-square response to nonstationary models can also be obtained similarly from equation 13 although the integration involved in the time domain is quite cumbersome. Bogdan-

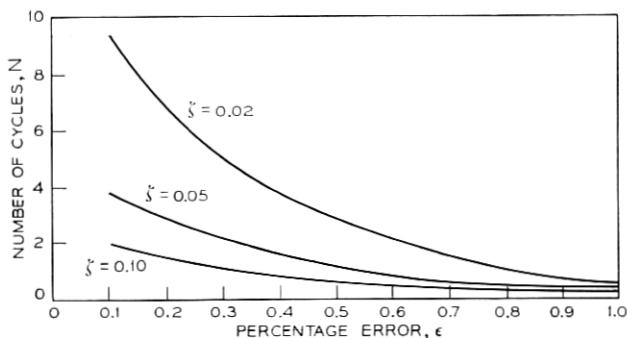


Fig. 6—Convergence of mean-square response of processes $x_1(t)$ and $x_2(t)$.

off, and others,⁹ have shown that

$$E[y_4^2(t)] = \frac{1}{p^2} \exp(-2\zeta\omega_n t) \sum_1^n \frac{a_i^2 \gamma_i(t)}{\chi_i^2} \quad (20)$$

where $\gamma_i(t)$ and χ_i are both functions of α_i , ω_i , and p .

Sometimes it is more convenient to calculate the mean-square response by integration in the frequency domain than in the time domain. For example, Brown¹⁷ has generalized Miller's¹⁸ result for the process $x_5(t)$ to the case where $\phi(t)$ is bounded on $(-\infty, \infty)$ and integrable on every finite subinterval of $(-\infty, \infty)$. His frequency formulation is

$$\text{Cov}_{y_5}(t_1, t_2) = \frac{1}{2\pi} \int_{-\infty}^{\infty} B(\omega, t_1) B^*(\omega, t_2) S_f(\omega) d\omega \quad (21)$$

$$E[y_5^2(t)] = \frac{1}{8\pi^3} \int_{-\infty}^{\infty} \left| \int_{-\infty}^{\infty} H(\omega_1) \Phi(\omega_1 - \omega_2) \exp(i\omega_1 t) d\omega_1 \right|^2 S_f(\omega_2) d\omega_2 \quad (22)$$

where $H(\omega)$, $\Phi(\omega)$, and $B(\omega, t)$ are the Fourier transforms of $h(t)$, $\phi(t)$, and $h(t - \tau)\phi(\tau)$, respectively, and the star denotes the complex conjugate. Barnoski and Maurer,¹⁹ using equation (21), evaluated $E[y_5^2(t)]$ numerically for cases where $\phi(t)$ is the unit step and rectangular functions and $f(t)$ is both white noise and noise with an exponentially decaying harmonic correlation function, that is, $R_f(\tau) = A \exp(-a|\tau|) \cos b\tau$. It was shown for white noise modulated by a unit step function that the system mean-square response will not exceed its stationary value for white noise. For correlated noise modulated in this same way, the system mean-square response may overshoot its stationary value. Note from equations (13) and (21) that

$$g_5(\tau, \tau') = \text{Cov}_{y_5}(\tau, \tau').$$

Substitution of this relation into equation (12) yields

$$\begin{aligned} E[y_5^2(t)] &= \int_{\Gamma} \int_{\Gamma} h(t - \tau) h(t - \tau') \text{Cov}_{y_5}(\tau, \tau') d\tau d\tau' \\ &= \frac{1}{p^2} \int_{\Gamma} \int_{\Gamma} \exp(\zeta\omega_n(\tau + \tau')) \sin p(t - \tau) \sin p(t - \tau') \\ &\quad \cdot \text{Cov}_{y_5}(\tau, \tau') d\tau d\tau'. \end{aligned} \quad (23)$$

Substitution of g_n in equation (13) into equation (12) yields

$$\begin{aligned} E[y_7^2(t)] &= \frac{1}{2p^2} \exp(-2\zeta\omega_n t) \int_{\Gamma} I(\tau) \exp(2\zeta\omega_n \tau) d\tau \\ &\quad - \int_{\Gamma} I(\tau) \exp(2\zeta\omega_n \tau) \cos p(t - \tau) d\tau. \end{aligned} \quad (24)$$

Using the relation $g_s(\tau, \tau') = \text{Cov}_{v\tau}(\tau, \tau')$ and letting $h_0(t)$ with parameters ω_0 , ζ_0 , and p_0 be of the same form as $h(t)$ in equation (11), it can be shown that

$$\begin{aligned}
 E[y_s^2(t)] &= \frac{1}{2p^2 p_0^2} \exp(-2\zeta\omega_n t) \\
 &\cdot \int_{\Gamma} \int_{\Gamma} \left\{ \exp[(\zeta\omega_n - \zeta_0\omega_0)(\tau + \tau')] \sin p(t - \tau) \sin p(t - \tau') \right. \\
 &\cdot \left[\cos p_0(\tau - \tau') \int_{\Gamma} I(\theta) \exp(2\zeta_0\omega_0\theta) d\theta \right. \\
 &\left. \left. - \int_{\Gamma} I(\theta) \exp(2\zeta_0\omega_0\theta) \cos p_0(\tau + \tau' - 2\theta) d\theta \right] \right\} d\tau d\tau'. \quad (25)
 \end{aligned}$$

It should be noted that, in equations (24) and (25), $I(\tau) = E[a^2(\tau)]\beta(\tau)$.

The mean-square response to linear first-order moving average and autoregressive processes (assuming a sampling interval Δt) for first-order and second-order filters are also found. Let the transfer function for the first-order filter be $h(t) = \exp(-a_0 t)$ (corresponding to a differential operator $p = d/dt + a_0$) and that for the second-order system be as given in equation (9), we obtain for the first-order ma process

$$E[y^2(t)] = \frac{c}{2a_0} [(1 + \theta_1^2) - q\theta_1](1 - \exp(-2a_0 t)), \quad (26)$$

(first-order filter);

$$\begin{aligned}
 E[y^2(t)] &= \frac{c}{2p^2} \exp(-2\zeta\omega_n t) \\
 &\cdot \left\{ (1 + \theta_1^2) \left[\frac{1}{2\zeta} (\exp(2\zeta\omega_n t) - 1) - \frac{\zeta}{2} \exp(2\zeta\omega_n t) \right. \right. \\
 &\left. \left. + \zeta \cos 2pt - (1 - \zeta^2)^{\frac{1}{2}} \sin 2pt \right] \right. \\
 &\left. + \theta_1 \left[(1 - \zeta^2)^{\frac{1}{2}} \sin 2pt - \zeta \cos 2pt \right. \right. \\
 &\left. \left. + \zeta \exp(2\zeta\omega_n t) + \frac{1}{\zeta} (1 - \exp(2\zeta\omega_n t)) \right] \right\}, \quad (27)
 \end{aligned}$$

(second-order filter);

and for first-order ar process

$$E[y^2(t)] = \frac{1}{1 - \theta_1^2} \frac{[1 - (\phi_1 \exp(a_0))^{-t}][(\exp(-a_0)\phi_1)^t - 1]}{(\ln \phi_1)^2 - a_0^2}, \quad (28)$$

(first-order filter);

$$E[y^2(t)] = \frac{[\exp(-a_1 t)(-a_1 \sin pt - p \cos a_1 t) + p]}{(1 - \phi_1^2)p^2(a_1^2 + p^2)(a_2^2 + p^2)} \cdot \frac{[\exp(-a_2 t)(-a_2 \sin pt - p \cos a_2 t) + p]}{(1 - \phi_1^2)p^2(a_1^2 + p^2)(a_2^2 + p^2)}, \quad (29)$$

(second-order filter).

In the above

$$c = \Delta t E[g_i^2],$$

$$q = 2 \exp(a_0 \Delta t),$$

$$a_1 = \zeta \omega_n + \ln \phi_1,$$

$$a_2 = \zeta \omega_n - \ln \phi_1.$$

It follows from equations (26) and (27) that the mean-square response to the first-order ma process approaches a steady-state value

$$\lim_{\substack{\Delta t \rightarrow 0 \\ t \rightarrow \infty}} E[y^2(t)] = \frac{c}{2a_0} (1 - \theta_1)^2, \quad \text{(first-order filter);} \quad (30)$$

$$= \frac{c(1 + \theta_1^2)}{4\omega_n^3 \zeta}, \quad \text{(second-order filter).} \quad (31)$$

Similarly from equations (28) and (29)

$$\lim_{\substack{\Delta t \rightarrow 0 \\ t \rightarrow \infty}} E[y^2(t)] = \frac{1}{(1 - \phi_1^2)[a_0^2 - (\ln \phi_1)^2]}, \quad \text{if } 0 < \phi_1 \leq 1, \quad (32)$$

(first-order filter);

$$= \frac{1}{(1 - \phi_1^2)\{[(\ln \phi_1)^2 + \omega_n^2]^2 - 4\zeta^2 \omega_n^2 (\ln \phi_1)^2\}}, \quad (33)$$

(second-order filter).

The above results indicate that the mean-square response of linear systems to either of the ar and ma processes approaches a certain stationary value when the time of passage is sufficiently long.

IV. CONCLUSIONS

When selecting a stochastic model it is important to consider not only the matching of statistical characterizations of real-world random data to those of the model, but also the effects of the model on vulnerable structural systems. The statistical characterizations are provided by joint probability distribution functions of the process conditioned on its duration and intensity. Ordinary power spectra and time-variable spectra such as the running spectrum

$$S(i\omega, t) = \int_0^t x(\tau) \exp(-i\omega\tau) d\tau$$

or the instantaneous spectrum

$$\rho(\omega, t) = \frac{\partial}{\partial t} |S(i\omega, t)|^2$$

can be used to characterize and form the simulation basis for the stationary and nonstationary processes, respectively. For the latter case, a second variable enters into the spectrum formulations and therefore complicates the analysis considerably. One alternative for analyzing nonstationary processes is to follow Priestley's theory of evolutionary processes and spectra.²⁰⁻²² Its applicability to ground motion and earthquakes will be investigated in a separate report. In general one must exercise engineering judgment upon consideration of the specific problem he studies in making an intelligent choice among all possible models. At the present time it appears that an earthquake ground-motion accelerogram can reasonably be treated as sectionally stationary when broken into three distinct phases. Each phase of the motion can be regarded as a short process and the corresponding power spectral density estimated by standard approaches to form the simulation bases for the $x_2(t)$ model. The applicability of this procedure is illustrated in Fig. 7 which shows the power spectrum densities associated with three distinct phases of recorded S21W ground motion during the Taft, California, 1952 earthquake. It is apparent from this earthquake that most of the input power to structures is provided by the midsection (from 3.3 to 13.6 seconds) of the motion. The power contained in low-intensity fluctuations preceding and following this stationary portion is relatively small.

Finally it should be pointed out that the stochastic models investigated in this paper can be easily realized by using a computer. The response statistics of these models are also reasonably easy to find. Although the

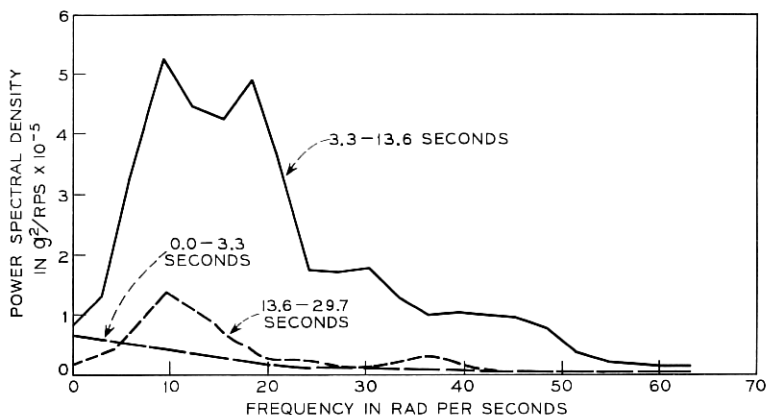


Fig. 7—Power spectral densities of Taft, California, S21W, July 21, 1952 earthquake.

current study is concerned primarily with ground-motion simulation, the results obtained can be applied also to many other engineering problems when time series modeling is required.

REFERENCES

1. Liu, S. C., "Statistical Analysis and Stochastic Simulation of Ground Motion Data," B.S.T.J., 47, No. 10 (December 1968), pp. 2273-2298.
2. Bycroft, G. N., "White Noise Representation of Earthquakes," Proc. Amer. Soc. Civil Engineers, 86, No. EM2 (April 1960), pp. 1-16.
3. Housner, G. W., and Jennings, P. C., Jr., "Generation of Artificial Earthquakes," Proc. Amer. Soc. Civil Engineers, 90, No. EM1 (February 1964), pp. 113-150.
4. Liu, S. C., and Jhaveri, D. P., "Spectral Simulation and Earthquake Site Properties," J. of Eng. Mech. Div., Proc. Amer. Soc. Civil Engineers, 95, No. EM-5 (October 1969), pp. 1145-1168.
5. Franklin, J. N., "Numerical Simulation of Stationary and Nonstationary Gaussian Random Processes," SIAM Review, 7, No. 1 (January 1965), pp. 68-80.
6. Leneman, O. A. Z., "Random Sampling of Random Processes: Impulse Processes," Inf. and Contr., 9, No. 6 (August 1966), pp. 347-363.
7. Beutler, F. J., and Leneman, O. A. Z., "The Spectral Analysis of Impulse Processes," Inf. and Contr., 12, No. 3 (March 1968), pp. 236-258.
8. Moore, J. B., and Anderson, B. D. O., "Simulation of Stationary Stochastic Processes," Proc. IEEE, 115, No. 2 (February 1968), pp. 337-339.
9. Bogdanoff, J. L., Goldberg, J. E., and Bernard, M. C., "Response of a Simple Structure to a Random Earthquake Type Disturbance," Bull. Seismological Soc. Amer., 54, No. 1 (February 1964), pp. 263-276.
10. Peterson, H. C., and Pullen, C. L., "Response of a Dynamic System to a Separable Nonstationary Random Excitation," J. Spacecraft Rockets, 3, No. 8 (August 1966), pp. 1299-1300.
11. Pullen, C. L., and Peterson, H. C., "Spectral Analysis of the Transient Response of a System to Random Excitation," Trans. Amer. Soc. Mech. Engineers, J. Appl. Mech., 33, Series E, No. 3 (September 1966), pp. 700-702.
12. MacNeal, R., Barnoski, R. L., and Bailie, J. A., "Response of a Simple Oscillator to Nonstationary Random Noise," J. Spacecraft Rockets, 3, No. 3 (March 1966), pp. 441-443.

13. Shinozuka, M., and Sato, Y., "Simulation of Nonstationary Random Process," *Proc. Amer. Soc. Civil Engineers*, 93, No. EM1 (February 1967), pp. 11-40.
14. Jennings, P. C., Housner, G. W., and Tsai, N. C., "Simulated Earthquake Motions," *Tech. Rept., Earthquake Engineering Research Lab., Calif. Inst. Tech., Pasadena, California*, April 1968.
15. Amin, M., and Ang, A. H. S., "A Nonstationary Model for Strong Motion Earthquakes," *Proc. Amer. Soc. Civil Engineers*, 94, No. EM2 (April 1968), pp. 559-583.
16. Caughey, T. K., and Stumpf, H. J., "Transient Response of a Dynamic System Under Random Excitation," *J. Appl. Mech., Trans. Amer. Soc. Mechanical Eng.*, 28, No. E-4 (December 1961), pp. 563-566.
17. Brown, J. L., "A Correlation Result for Nonstationary Inputs," *Quart. Appl. Math.*, 24, No. 1 (April 1966), pp. 93-95.
18. Miller, K. S., "A Note on Input-Output Spectral Densities," *Quart. Appl. Math.*, 21, No. 1 (October 1963), pp. 249-252.
19. Barnoski, R. L., and Maurer, J. R., "Mean-Square Response of Simple Mechanical System to Nonstationary Excitation," *J. Appl. Mech., Trans. Amer. Soc. Mechanical Eng.*, 36, Series E, No. 2 (June 1969), pp. 221-228.
20. Priestley, M. B., "Evolutionary Spectra and Nonstationary Processes," *J. R. Statist. Soc. B.*, 27, No. 2 (1965), pp. 204-237.
21. Priestley, M. B., "Power Spectral Analysis of Non-stationary Random Processes," *J. Sound Vib.*, 6, No. 1 (July 1967), pp. 86-97.
22. Priestley, M. B., and Rao, T. S., "A Test for Non-stationarity of Time-series," *J. R. Statist. Soc. B*, No. 1 (1969), pp. 140-149.

